Supplemental Information

A comprehensive optogenetic pharmacology toolkit for *in vivo* control of $GABA_A$ receptors and synaptic inhibition

Wan-Chen Lin,[1,2] Ming-Chi Tsai,[1,2] Christopher M. Davenport,[1] Caleb M. Smith,[1] Julia Veit,[1] Neil M. Wilson,[1] Hillel Adesnik,[1] and Richard H. Kramer[1,*]

[1]Department of Molecular and Cell Biology, University of California, Berkeley, CA 94720, USA
[2]Co-first authors
[*]Correspondence: rhkramer@berkeley.edu

Supplemental Figures

Figure S1, related to Figure 1. Illustrates the design principles of LiGABARs presented in this work. Also provides one representative dataset of receptor screening.

Figure S2, related to Figure 1. Demonstrates that receptor functions are not affected by cysteine mutation or PTL conjugation. Also provides the GABA concentration used for measuring LiGABAR photosensitivity for each α-isoform.

Figure S3, related to Figure 1. Demonstrates that PTL treatment does not photosensitize endogenous ion channels, including the wild-type $GABA_A$ receptors, in a neuron.

Figure S4, related to Figure 2. Demonstrates that LiGABAR photoswitching can be orthogonal to two-photon GABA uncaging.

Figure S5, related to Figure 3. Demonstrates that exogenously expressing a cysteine-substituted α-subunit of $GABA_A$ receptor does not affect neuronal excitatory-inhibitory balance or the kinetics of inhibitory postsynaptic currents.

Figure S6, related to Figure 7. Illustrates the gene targeting strategy for generating the α1-$GABA_A$ PhoRM knock-in mouse.

Figure S7, related to Figure 8. Illustrates the analysis and categorization of data from multi-electrode recordings.

Supplemental Experimental Procedures

Supplemental References

Supplemental Figures

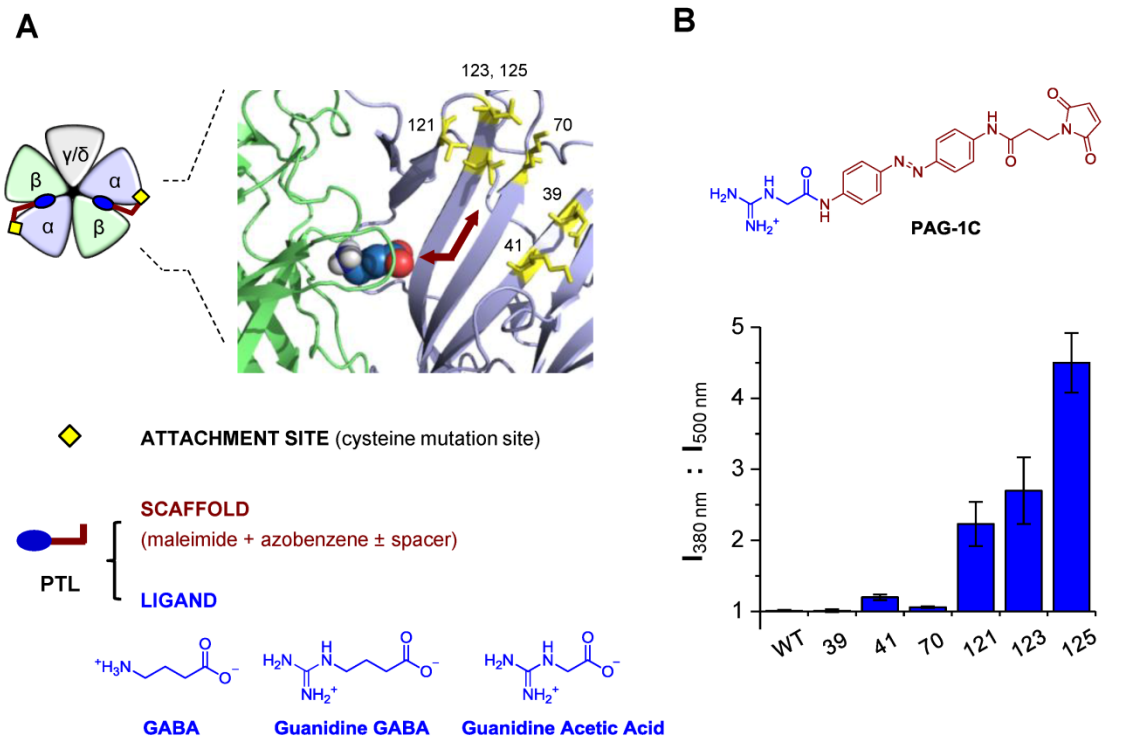

Figure S1. The design and screening of new LiGABARs.

(A) The chemical modules comprising a photoswitchable tethered ligand (PTL) and the proposed model of PTL-mediated receptor antagonism. The top panel illustrates a LiGABAR occupied by its conjugated PTL. PTL conjugation is achieved via a Michael-addition reaction between the maleimide (of the PTL) and the sulfhydryl group (of the cysteine residue). Putative PTL conjugation sites (yellow sticks; i.e. residues subject to cysteine substitution) on the α1-subunit (blue ribbon) are shown in a homology model (O'Mara et al., 2005). The docking of GABA (spheres) in this receptor model suggests that the carboxyl group of GABA faces toward the complementary face of the α1-subunit. Thus an optimized scaffold (maleimide + *cis* or *trans* azobenzene ± spacer; thick brown arrow in the model) can efficiently deliver the ligand moiety (GABA or its analogue) into the binding pocket once conjugated at an appropriate location. The new PTLs are soluble in water due to their positive charges formed at physiological pH. Note that the negatively charged carboxylate groups (at physiological pH) of the free ligands will be converted into neutral amide groups in the PTLs. Because this negative charge is critical for receptor activation, the tethered ligands are expected to antagonize rather than activate the receptor. Finally, the guanidinium groups of GABA analogues are expected to form more ionic and/or hydrogen-bond interactions inside the binding pocket, compared to the ammonium group of GABA, and enhance receptor antagonism. The optimal LiGABARs (PTL+mutant) for individual α-isoforms are listed in Figures 1E and 1F.

(B) Screening of PAG-1C conjugation sites for the α1-isoform. The α1 subunit (wild-type or one of the six cysteine-substituted mutants indicated in panel A) was co-assembled with β2 and γ2S subunits in HEK cells, and the cells were treated with PAG-1C prior to electrophysiological evaluations. Currents elicited by 10 μM GABA in either 380 nm or 500 nm light were recorded. Photosensitivity of PAG-1C treated receptors was indexed as the ratio of peak current amplitude in 380 nm vs. in 500 nm (i.e. I_{380nm}/I_{500nm}). A ratio of 1 indicates that the treated receptor was not functionally affected by light switching. The results show that receptor photosensitization requires not only the presence but also the proper location of a cysteine in the α1 subunit. Whole-cell voltage-clamp recordings were carried out with cells held at –70 mV. Data are plotted as mean ± SEM (n = 3–6).

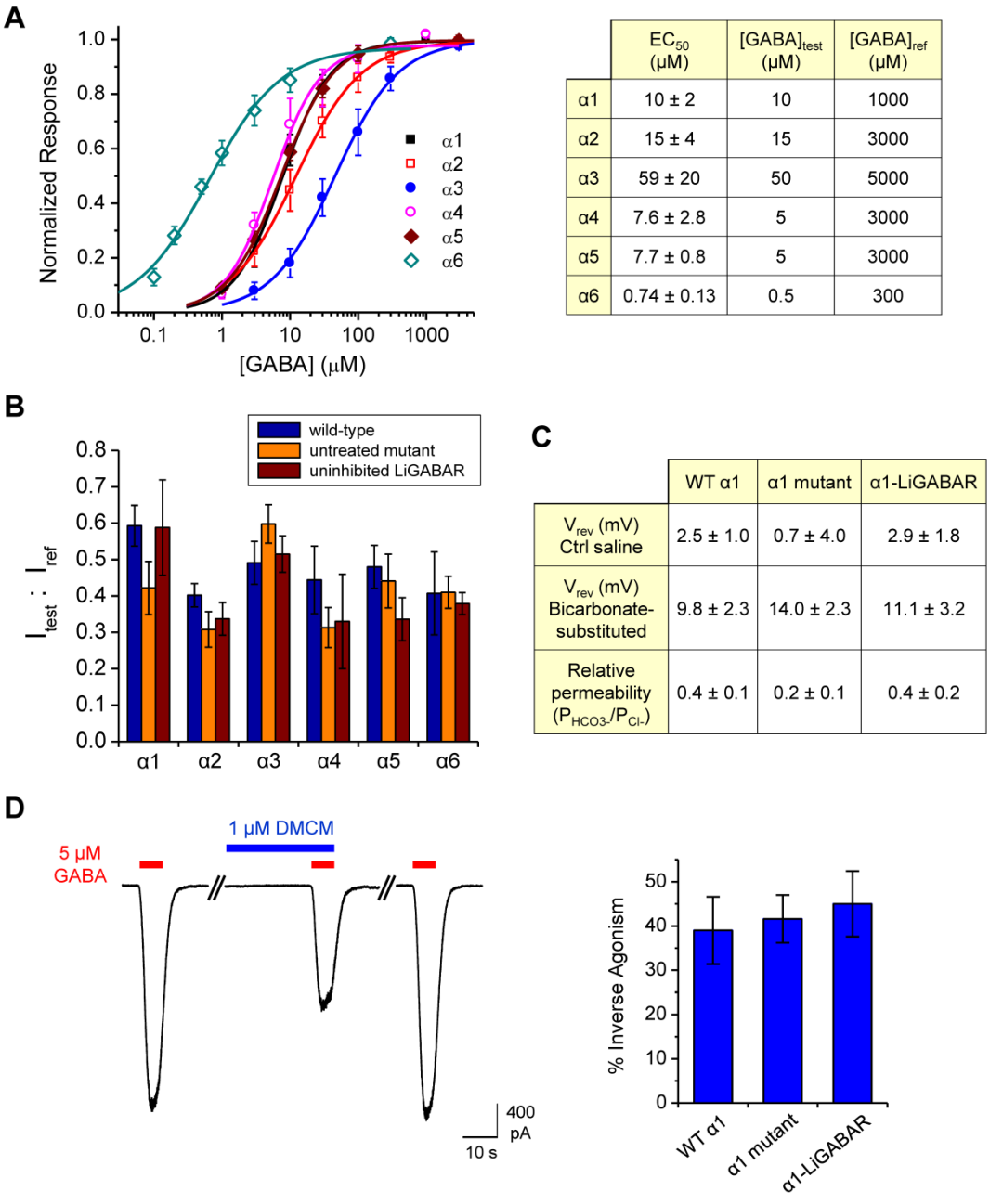

	EC_{50} (μM)	$[GABA]_{test}$ (μM)	$[GABA]_{ref}$ (μM)
α1	10 ± 2	10	1000
α2	15 ± 4	15	3000
α3	59 ± 20	50	5000
α4	7.6 ± 2.8	5	3000
α5	7.7 ± 0.8	5	3000
α6	0.74 ± 0.13	0.5	300

	WT α1	α1 mutant	α1-LiGABAR
V_{rev} (mV) Ctrl saline	2.5 ± 1.0	0.7 ± 4.0	2.9 ± 1.8
V_{rev} (mV) Bicarbonate-substituted	9.8 ± 2.3	14.0 ± 2.3	11.1 ± 3.2
Relative permeability (P_{HCO3-}/P_{Cl-})	0.4 ± 0.1	0.2 ± 0.1	0.4 ± 0.2

Figure S2. Receptor functions are not affected by cysteine mutation or PTL conjugation.

(A) Defining testing conditions based on the EC_{50} of GABA for wild-type receptors. The dose-response curve of each wild-type α-isoform (co-assembled with wild-type β2 and γ2S) is plotted by fitting the respective grouped data (mean ± SEM; n = 4–7) with Hill Equation. The GABA EC_{50} for each isoform is calculated as mean ± SEM from 4–7 individually analyzed cells. Details of data analysis are described in "Data Analysis" of the *Supplemental Experimental Procedures*. $[GABA]_{test}$, the concentration of GABA used for indexing LiGABAR photosensitivity (Figure 1E) and receptor activation (panel B, see below), was set to be ~EC_{50} of the wild-type receptor.

(B) Receptor activation is not affected by cysteine mutation or PTL conjugation. For each isoform, the impacts of receptor modifications were assayed by comparing the fraction of receptor activation at $[GABA]_{test}$ among the wild-type (blue), the untreated mutant (orange), and the PTL-conjugated mutant receptors (dark red; measured when the receptor was not photo-antagonized). The fraction of receptor activation is defined as the ratio of peak current amplitude at $[GABA]_{test}$ vs. at a saturating concentration (i.e. $[GABA]_{ref}$ in panel A). Data are plotted as mean ± SEM (n = 3–7). For α2 and α5, the PTL used for LiGABAR was PAG-1C. The p value for each α-isoform is >0.05 (two-tailed *t* test) when comparing the untreated mutant or uninhibited LiGABAR with the wild-type.
(C) Channel permeability to bicarbonate (relative to chloride) is not affected by cysteine mutation or PTL conjugation. The relative permeability (P_{HCO3-}/P_{Cl-}) through wild-type α1β2γ2S, α1(T125C)β2γ2S, and α1-LiGABAR (uninhibited) was measured in HEK cells using a previously described method (Wotring et al., 1999). In brief, reversal potential was measured in a modified saline with 75 mM of NaCl (of the control saline, i.e. regular extracellular solution) replaced by $NaHCO_3$. P_{HCO3-}/P_{Cl-} was calculated using a rearranged Goldman-Hodgkin-Katz equation: $P_{HCO3-}/P_{Cl-} = \{[Cl^-]_i exp(-V_{rev}F/RT) - [Cl^-]_o\}/[HCO3^-]_o$, where $[Cl^-]_i$ is the intracellular chloride concentration, V_{rev} is the reversal potential, $[Cl^-]_o$ is the extracellular chloride concentration, and $[HCO3^-]_o$ is the extracellular bicarbonate concentration. F, R, T are Faraday's constant, gas constant, and temperature, respectively. The results show that the reversal potentials in control and modified saline, as well as P_{HCO3-}/P_{Cl-}, are not altered by cysteine mutation or PTL conjugation (p >0.05, two-tailed *t* test). Data are shown as mean ± SEM (n = 4–6).
(D) Receptor modulation through the benzodiazepine site is not altered by cysteine mutation or PTL conjugation. (left) Representative recording traces showing receptor inhibition mediated by DMCM, an inverse agonist targeting the benzodiazepine site. A 20-s pre-application of DMCM was carried out prior to the co-application of GABA and DMCM. When testing on α1-LiGABAR, a 5-s flash of 380 nm light was illuminated before the application of GABA or DMCM (to relieve LiGABAR from photo-antagonism). (right) Group data (mean ± SEM; n = 4–5) showing that there is no difference in DMCM-mediated inverse agonism between wild-type α1β2γ2S, α1(T125C)β2γ2S, and α1-LiGABAR (p >0.05, two-tailed *t* test).

Recordings for panels A, B, and D were carried out in HEK-293 cells held at –70 mV.

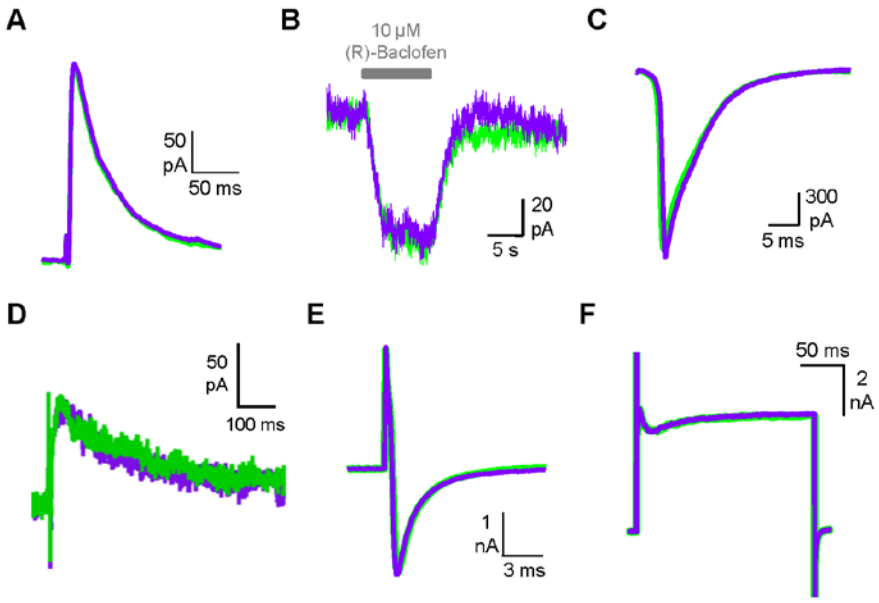

Figure S3. PTL treatment does not confer light sensitivity onto endogenous ion channels in hippocampal neurons.

(A) PAG-1C treatment does not photosensitize endogenous $GABA_A$ receptors in hippocampal slices. Representative evoked IPSC traces are shown. I_{500}/I_{380} = 1.00 ± 0.03 (in peak amplitude; V_{hold} = 0 mV; n = 5, p = 0.89).
(B) PAG-1C treatment does not photosensitize endogenous $GABA_B$ receptors in cultured hippocampal neurons. Representative GIRK currents elicited by 10 µM (*R*)-baclofen are shown. I_{500}/I_{380} = 1.00 ± 0.04 (V_{hold} = –70 mV; n = 4, p = 0.90).
(C) PAG-1C treatment does not photosensitize endogenous AMPA receptors in hippocampal slices. Representative evoked EPSC traces are shown. I_{500}/I_{380} = 1.01 ± 0.01 (in peak amplitude; V_{hold} = –60 mV; n = 4, p = 0.16).
(D) PAG-1C treatment does not photosensitize endogenous NMDA receptors in hippocampal slices. Representative evoked EPSC traces are shown. I_{500}/I_{380} = 0.97 ± 0.05 (in peak amplitude; V_{hold} = +40 mV; n = 3, p = 0.59).
(E) PAG-1C treatment does not photosensitize endogenous voltage-gated Na^+ channels in hippocampal slices. Representative inward currents (elicited by a 200-ms depolarization step from –60 to –10 mV) are shown. I_{500}/I_{380} = 1.00 ± 0.01 (in peak amplitude; n = 11, p = 0.72).
(F) PAG-1C treatment does not photosensitize endogenous voltage-gated K^+ channels in hippocampal slices. Representative outward currents (elicited by a 200-ms depolarization step from –60 to +40 mV) are shown. I_{500}/I_{380} = 0.997 ± 0.0041 (steady-state amplitude; n = 5, p = 0.41).

Recordings for panels A, C, D, E, and F were carried out in CA1 pyramidal neurons. Recording traces acquired under 380 nm and 500 nm illumination are plotted in purple and green, respectively. Group data of I_{500}/I_{380} are reported as mean ± SEM, and p values were calculated from two-tailed *t* tests. Additional details of PTL treatment and electrophysiology are described in the *Supplemental Experimental Procedures*.

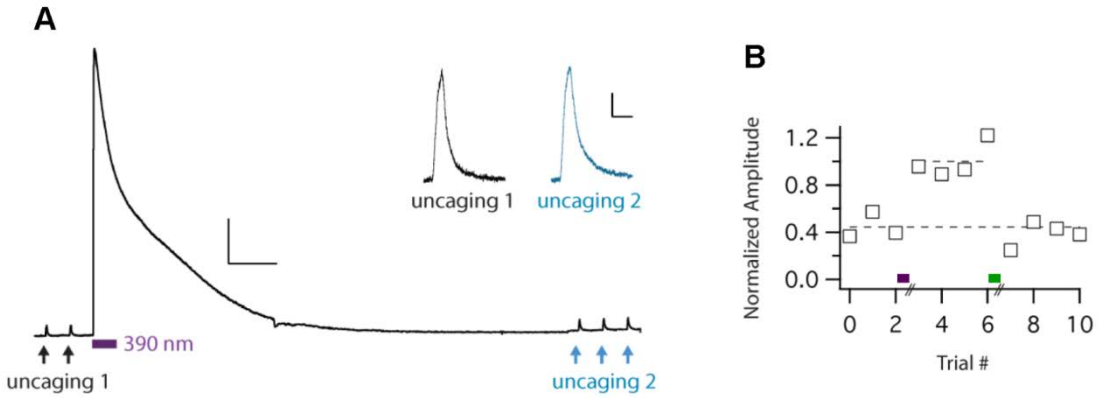

Figure S4. LiGABAR photoswitching can be paired with two-photon GABA uncaging.

(A) Conditioning light for LiGABAR photoswitching can be orthogonal to GABA uncaging. Whole-cell voltage-clamp recordings were carried out from hippocampal pyramidal neurons held at 0 mV, in the presence of 25 μM DNQX, 50 μM AP5, and 0.5 μM TTX. Responses to two-photon photolysis of RuBi-GABA (by 800 nm) were identical before (back arrows) and after (blue arrows) a conditioning flash (390 nm; purple bar). I_{after}/I_{before} = 1.02 ± 0.03, n = 4 cells, p = 0.65. The conditioning flash caused some photolysis of RuBi-GAGA, but the released GABA can diffuse away in 0.5–2 min after the flash. Scale bars = 500 pA, 1 s. (inset) Magnification of uncaging responses before (black) and after (blue) conditioning flash. Scale bars = 25 pA, 500 ms.
(B) Two-photon illumination for GABA uncaging does not affect the state of the LiGABAR. Current amplitudes from an example cell over multiple trials in response to RuBi-GABA photolysis. Response amplitude was stable after photo-antagonism was relieved (by a 390-nm conditioning flash (purple bar); I_{last}/I_{first} = 0.94 ± 0.06, n = 6 cells, p = 0.35) or triggered (by a 540-nm conditioning flash (green bar); I_{last}/I_{first} = 1.01 ± 0.03, n = 6 cells, p = 0.89). Currents are normalized to the mean amplitude after 390 nm illumination. Whole-cell voltage-clamp recordings were carried out from hippocampal pyramidal neurons expressing α5-LiGABAR (conjugated with PAG-1C; *trans*-antagonism). Cells were held at 0 mV and treated with 25 μM DNQX, 50 μM AP5, and 0.5 μM TTX.

I_{after}/I_{before} (panel A) and I_{last}/I_{first} (panel B) are reported as mean ± SEM; p values are calculated from two-tailed *t* tests.

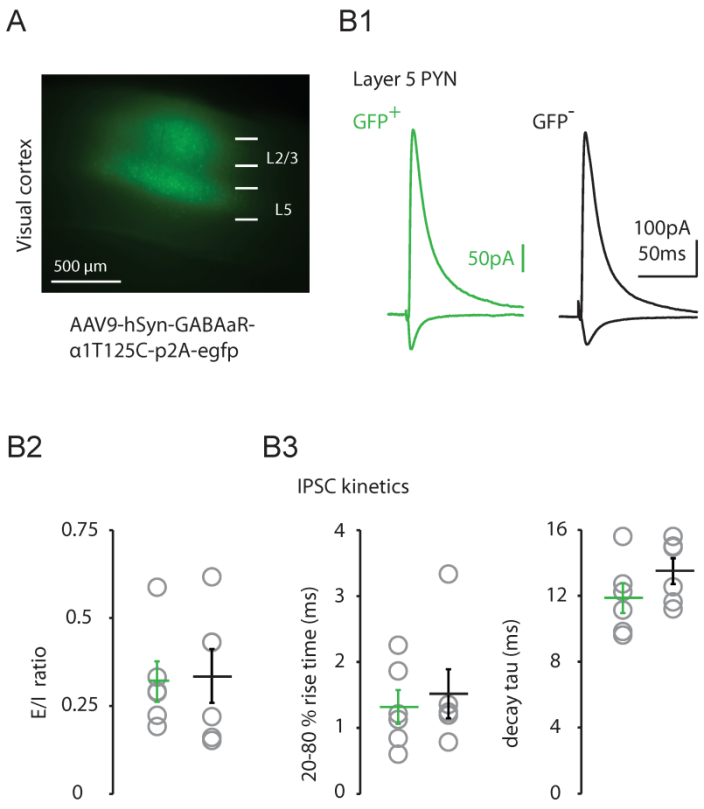

Figure S5. Exogenously expressing a cysteine mutant of $GABA_A$ receptors does not significantly change neuronal excitability or the kinetics of inhibitory postsynaptic currents.

(A) Fluorescence image of a cortical slice prepared from a mouse injected with a bi-cistronic AAV encoding α1T125C and eGFP. Virally infected neurons were identified by the green fluorescence.
(B1) Recording traces from layer 5 pyramidal neurons expressing (GFP+) or not expressing (GFP–) α1T125C. Postsynaptic excitatory and inhibitory currents were evoked by electrical stimulation, with each neuron voltage-clamped at –65 mV and 0 mV, respectively.
(B2) The ratio of excitatory vs. inhibitory currents (E/I ratio; mean ± SEM) in α1T125C-expressing neurons (green; 0.32 ± 0.06, n = 6) is not significantly different from that in control neurons (black; 0.34 ± 0.08, n = 6; $p > 0.05$, two-tailed *t* test).
(B3) IPSCs in α1T125C-expressing neurons (green) and control neurons (black) showed no significant differences in either the rise time or decay time constant. GFP+ vs. GFP– neurons: 20-80% rise time, 1.32 ± 0.26 ms vs. 1.52 ± 0.37; decay time constant, 11.9 ± 0.9 ms vs. 13.5 ± 0.8 ms, n = 6 and 6, respectively; $p > 0.05$, two-tailed *t* test.

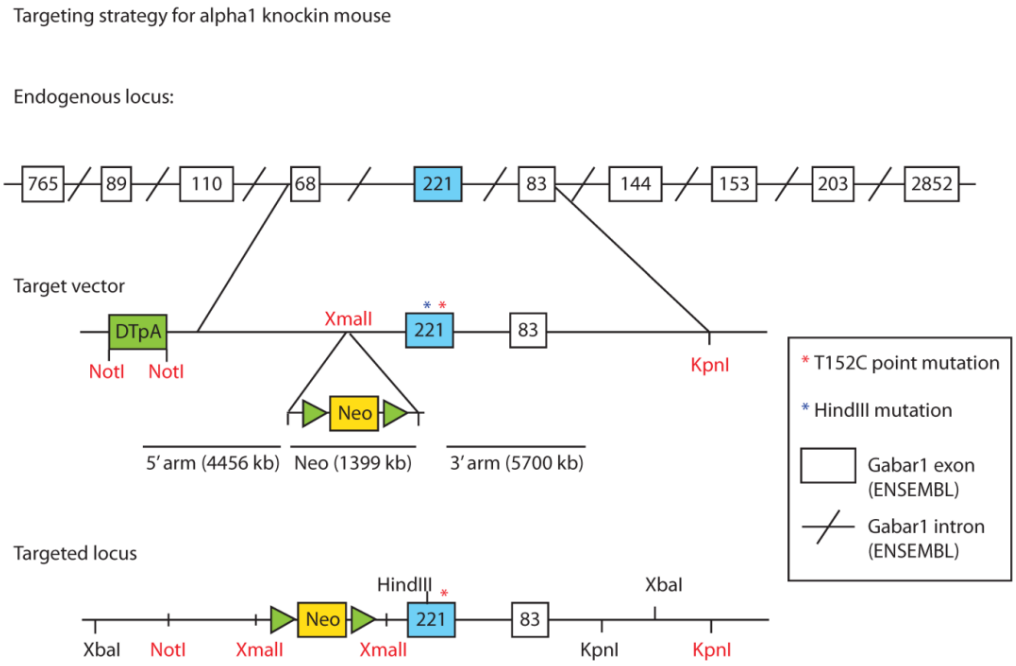

Figure S6. Strategy of gene targeting for generating the α1T125C knock-in mouse.

The genomic region of *Gabra1* (NM_010250.4) was obtained from BAC clone RPCI-24 and was used to develop a targeting vector that contains the genomic region surrounding exons 5 and 6 of *Gabra1*. A cysteine mutation was introduced to T152 (counting from the start codon, i.e. T125 in the mature peptide sequence) on exon 5 as well as a C to T silent mutation to create a Hind III site upstream of T152C for genotyping. A loxP site flanked neomycin gene and a diphtheria toxin A-chain (DTpA) gene were introduced in the targeting vector upstream of exon 5 for positive-negative ES cell selection.

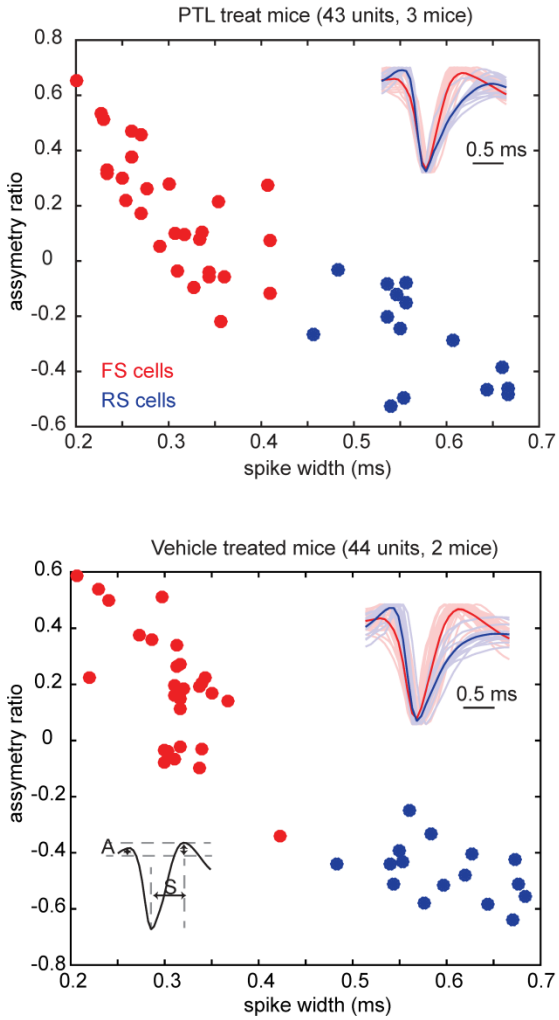

Figure S7. Separation of FS and RS neurons.

We used *k*-means clustering to categorize all of the recorded units. Top and bottom panels show the scatter plot of the spike width and the asymmetry ratio from all units recorded in PTL-treated and vehicle-treated knock-in mice, respectively. Inset in the bottom left illustrates the definition of spike width (S) and amplitude (A) of peaks to construct the plot (detailed in *Data analysis* section). The average waveforms of all FS (red) or RS (blue) units in each group are shown in the top and bottom right insets. In the PTL group, FS and RS cells have S of 0.30 ± 0.021 and 0.57 ± 0.043 ms, respectively. In the vehicle group, FS and RS cells have S of 0.31 ± 0.016 and 0.60 ± 0.037 ms, respectively. Data are mean ± SEM

Supplemental Experimental Procedures

Unless otherwise indicated, chemicals and buffers were obtained from Sigma, Tocris, or Thermo-Fisher Scientific. All experiments were performed in accordance to the guidelines and regulations of the ACUC at the University of California, Berkeley.

Cloning and Virus Preparation

The cDNAs of wild-type rat $GABA_AR$ α1 (in pGH19), α2 (in pRK7), α3 (in pRK7), β2 (in pGH19), and γ2S (in pUNIV) were obtained from Professor Cynthia Czajkowski (University of Wisconsin, USA). The cDNAs of wild-type rat $GABA_AR$ α4 and α6 (both in pCMVNeo) were obtained from Professor Robert L. Macdonald (Vanderbilt University, USA). The pGH19 clones of wild-type α1 and β2 subunits were sub-cloned into vector pCDNA3.1 for expression in HEK293 cells. The wild-type rat $GABA_AR$ α5 in vector pRK5 was obtained from Dr. Hartmut Luddens (University of Mainz, Germany) and was then sub-cloned into vector pCDNA3.1 for further processing. Cysteine mutants of α-subunits were prepared by site-directed mutagenesis in the wild-type clones, and the mutations were confirmed by sequencing. The mutants used in the LiGABAR toolkit are (numbered based on the mature sequence): α1T125, α2Q121, α3V146, α4M120, α5E125, and α6M120 (if counted from the start codon: α1T152, α2Q149, α3V174, α4M155, α5E156, and α6M139).

The cDNA of GFP-fused intrabody against gephyrin (GPHN.FingR-GFP in vector pCAG; Gross, et al., 2013) was a gift from Prof. Don Arnold at the University of Southern California, USA (Addgene plasmid # 46296).

For neuronal expression, bi-cistronic pAAV constructs encoding a mutant α-subunit (α1T125C or α5E125C) and an eGFP marker were prepared following the previously published procedures (Lin et al., 2014). Each mutant α-subunit has an N-terminal *myc* epitope tag which does not affect receptor function and synaptic targeting (Connolly, et al., 1996; Tretter et al., 2008). Gene expression is conferred by a human synapsin-1 promoter (Kugler et al., 2003). The resulting DNA clones were subsequently packaged into AAV9 at a titer of 10^{12}–10^{13} vg/mL.

Animals

Pregnant female mice for neonatal viral injection (see below) and Sprague-Dawley rats were obtained from Charles River Laboratories. PV-tdTOM mice were derived from crossing the two following mouse lines: PV-CRE (Jackson lab stock #008069) and Rosa-LSL-tdTOMATO (Allen Institute line Ai9, Jackson Labs #007905).

α1T125C knock-in mice were generated via UC Davis mouse biology program. The genomic region of *Gabra1* (NM_010250.4) was obtained from BAC clone RPCI-24 and was used to develop a targeting vector that contains the genomic region surrounding exons 5 and 6 of *Gabra1*. We introduced a cysteine mutation for T152 (counting from the start codon) on exon 5

as well as a C to T silent mutation to create a Hind III site upstream of T152C for genotyping. The final targeting construct is shown in Figure S6. The construct was linearized and electroporated into ES cells from mouse strain 129. Cells were selected for transmitted neomycin resistance and homologous recombination was confirmed on flanking regions of the targeting vector. A loss of allele assay was performed to confirm a single recombination event. After karyotyping, ES cells were injected into C57/B6 mouse blastocysts and implanted into surrogates resulting in chimeras. After confirming germline transmission the F2 offspring were bred with a Cre recombinase expressing mouse to excise the neomycin cassette. The resulting progeny were bred to homozygosity of the *Gabra1* knock-in and the Cre cassette was bred out.

Culture and Transfection of HEK cells

Cells were maintained in Dulbecco's Minimum Essential Medium (Gibco) supplemented with 10% fetal bovine serum (Gibco) at 37 ˚C and 5% CO_2. Cells were seeded in a 24-well plate (20–25 × 10^3 cells/well) on 12-mm poly-L-lysine coated coverslips and were transfected by calcium phosphate precipitation at 40–50% confluence. A total of ~1.1 µg DNA per coverslip was used. For α1, α2, α3, and α5, the DNA mixture comprised (µg): 0.15 α, 0.15 β, 0.75 γ, and 0.05 eGFP. For α4 and α6, the DNA mixture comprised (µg): 0.25 α, 0.25 β, 0.50 γ, and 0.05 eGFP. Cells were used 1–2 days after transfection.

Culture and Transfection of Dissociated Hippocampal Neurons

Cultures of dissociated hippocampal neurons were prepared from P0–P2 neonatal rats. In brief, pups were decapitated and the brains were removed to warmed HBSS++ solution (Ca^{2+}- and Mg^{2+}-free Hank's Balanced Salt Solution (Gibco) supplemented with 1 mM HEPES and 20 mM glucose). Hippocampi were dissected from brain and digested for 12 min in 0.25% trypsin (Gibco), washed five times in HBSS++ and transferred to warmed neural growth medium (NGM). NGM was made of Eagle's Minimum Essential Medium (Gibco) supplemented with 20 mM glucose, 5% FBS (Gibco), 1X B27 supplement (Gibco), 2 mM glutamine (Gibco), and serum extender (BD Biosciences). Hippocampi were then triturated with fire-polished Pasteur pipettes and passed through a 40-µm cell strainer to isolate individual cells. Cells were seeded in a 24-well plate (75–100 × 10^3 cells/well) on 12-mm poly-L-lysine coated coverslips, and were then maintained in NGM at 37 ˚C and 5% CO_2. Half of the culture medium was replaced with fresh NGM every 2–3 days. Cytosine arabinoside (araC; Sigma) was added on 4 DIV (to a final concentration of 2 µM in culture) to inhibit the proliferation of non-neuronal cells. On 7–9 DIV, neurons were transfected with α1(T125C) (in pCDNA3.1, 0.8 µg/well) and GPHN.FingR-GFP (in pCAG, 0.4 µg/well) via calcium phosphate precipitation. Two-photon uncaging experiments were carried out 5–10 days thereafter.

Preparation and Viral Transduction of Organotypic Slice Cultures (Hippocampus)

Postnatal day 8 Sprague-Dawley rat pups were anaesthetized and decapitated. Hippocampi were dissected and sliced into 350 µm-thick sections using a tissue chopper (Stoelting). Slices were

maintained at 34 ˚C on cell culture inserts (Milipore) in Neurobasal-A medium (Life Technologies) supplemented with 20% horse serum (Thermo Scientific), 0.03 units/mL insulin (Sigma), 0.5 mM ascorbic acid, 1X Gluta-Max (Life Technolgies), 80 units/mL penicillin (Life Technolgies), 80 µg/ml streptomycin (Life Technolgies), and 25 mM HEPES. One day after preparation, slices were injected with AAV9 encoding eGFP-2A-α1T125C or eGFP-2A-α5E125C. The CA1 pyramidal cell body layer was injected at 1–2 sites/slice with 150 nL of virus with a fine glass pipette. Slices were used 5–14 days post-injection.

Viral Expression of Mutant α-Subunits in the Mouse Visual Cortex

Stereotactic Injection. Three to four weeks old wide-type or PV-tdTOM mice were injected stereotactically with a bi-cistronic AAV (see "Virus Preparation" above). Mice were anesthetized with isoflurane and a small craniotomy was made for the insertion of a beveled injection needle (Drummond) at 2.5 mm lateral and 0.5 mm anterior to lambda. The pipette was slowly lowered to 150–250 µm below the brain surface. 120–150 nL of virus was injected over 4 min. The needle was left in place for an additional 2 min to allow viral diffusion. After removing the injection needle, the scalp was sutured. The animals were then given a dose of analgesics (buprenorphine, 0.1 mg/kg) and were allowed to recover for 2–3 weeks before the experiments. Infection was confirmed with an epifluorescent stereomicroscope and fluorescence was used to target all subsequent craniotomies and recordings *in vivo*.

Neonatal Injection. Neonates (P0–P3) of wild-type mice were anesthetized on ice, placed in a custom mold, and injected with 10–30 nL of virus at 1–2 sites in the visual cortex (1–1.5 mm lateral to lambda, 0 AP, 300–500 µm DV). Experiments were carried out ~3 weeks thereafter.

Preparation of Acute Brain Slices

Mice (3 weeks to 2 months old) of both sexes were used for slice preparation. For animals older than 1 month old, animals underwent intracardiac perfusion of ice cold cutting solution (see below) after katamine and xylazine induced anesthesia. Acute brain slices (350 µm) from either visual cortex or cerebellar vermis were prepared in ice-cold cutting solution containing (in mM): 85 NaCl, 2.5 KCl, 0.5 $CaCl_2$, 4 $MgCl_2$, 1.25 NaH_2PO_4, 25 $NaHCO_3$, 75 sucrose, 0.4 ascorbic acid and 25 glucose (saturated with 95% O_2 and 5% CO_2; pH 7.4). To record cerebellar Golgi cells, slices were prepared in (mM): 130 K-gluconate, 25 glucose, 15 KCl, 20 HEPES, 0.05 EGTA, and 1 kynurenic acid (Abcam), saturated with 95% O_2 and 5% CO_2; pH 7.4 (ice-cold). After sectioning, slices were transferred to a holding chamber containing artificial cereberospinal fluid (aCSF) containing (in mM): 119 NaCl, 2.5 KCl, 2.5 $CaCl_2$, 1.3 $MgCl_2$, 1 NaH_2PO_4, 26.2 $NaHCO_3$, and 11 glucose (saturated with 95% O_2 and 5% CO_2; pH 7.4) at 34 ˚C for 20 min and were then cooled down to room temperature. PTL treatment was carried out at room temperature thereafter (see below).

Ex vivo PTL Treatment

HEK cells and cultured neurons. Cells (in extracellular solution; see formula in the *Electrophysiology* section) were treated with tris(2-carboxyethyl)phosphine (TCEP; 2.5–5 mM, 5–10 min), washed, and then treated with PTL (25 µM, 25 min, pH 8.0 for HEK cells and 7.4 for cultured neurons) at room temperature.

Organotypic slices. Slices (in aCSF) were treated with TCEP (5 mM, 5 min), washed, and then incubated with PAG-1C (25–50 µM) and guanidinium hydrochloride (500 µM) for 60 min at room temperature.

Acute slices. Slices (in aCSF) were treated with TCEP (5 mM, 8–10 min), washed, and incubated with either PAG-1C (25–50 µM, with 500 µM guanidinium hydrochloride) or PAG-2A (25–50 µM) for >35 min at room temperature.

In vivo PTL Treatment

Custom-made chambers were implanted over the visual cortex of virus-injected or α1(T125C) knock-in mice. For experiments in Figures 5 and 6, we made a craniotomy of 2-3 mm in diameter with subsequent duratomy on anesthetized mice. We applied 100 µL of HEPES-aCSF (in mM: 125 NaCl, 3 KCl, 10 HEPES, 10 glucose, 2 $CaCl_2$, 2 $MgCl_2$; pH 7.4, 290 mOsm) containing PAG-1C (250 µM) and TECP (250-500 µM) onto the exposed cortex for 1 hr. The solution was then removed from the brain, and HEPES-aCSF was applied to rinse off residual drugs. The mice were either used in slice preparation (Figure 5) or covered with 1.5–2% low-melting temperature agarose (in HEPES-aCSF) on the brain for two-photon guided patching (Figure 6). For multi-electrode recording in awake knock-in mice (Figure 8), we thinned the skull and opened a small craniotomy (0.5–1.5 mm in diameter) without duratomy over the visual cortex. We infused the PTL solution into the brain at a rate of 100 nL/min for 10 min with a glass micropipette attached to a microinfusion pump (UMP3 with SYS-Micro4 controller; World Precision Instrument). The surgery lasted less than 40 min and recordings started at least 45 min after the mice recovered from anesthesia. In control experiments, vehicle solution containing 500 µM TCEP without PAG-1C was infused.

In vitro Electrophysiology

HEK cells. Recordings were carried out at room temperature using pipettes with 2.5–5 MΩ resistance. Cells were held at –70 mV. Pipettes were pulled from filamented borosilicate pipettes (G150TF-3, Sutter Instruments). The extracellular solution contained (in mM): 138 NaCl, 1.5 KCl, 1.2 $MgCl_2$, 2.5 $CaCl_2$, 5 HEPES, 10 Glucose; pH 7.4. The intracellular solution contained (in mM): 140 CsCl, 4 NaCl, 10 HEPES, 2 MgCl2, 2 Mg-ATP, and 10 EGTA; pH 7.2. Signals were amplified using a Patch Clamp PC-501A amplifier (Warner Instruments), low-pass filtered at 2 kHz, digitized at 10 kHz by a Digidata 1322A converter (Molecular Devices), and acquired with software Clampex 10 (Molecular Devices). Illumination for photo-control was

provided by a Lambda-LS xenon lamp (Sutter Instruments) with 379 ± 17 nm and 500 ± 8 nm band pass filters.

Two-photon uncaging at cultured hippocampal neurons. For the uncaging experiments in Figures 2H and 2I, whole-cell voltage-clamp recordings were carried out at room temperature in re-circulated aCSF containing (in mM): 126 NaCl, 2.5 KCl, 1.25 NaH_2PO_4, 10 Glucose, 1.3 $MgCl_2$, 26 $NaHCO_3$, 2.5 $CaCl_2$, 0.025 DNQX, 0.05 D-AP5, 0.0005 TTX, and 0.2–0.4 RuBi-GABA (Abcam) equilibrated with 95% O_2 + 5% CO_2. Neurons were held at 0 mV. The internal solution contained (in mM): 108 Cs-gluconate, 2.8 NaCl, 20 HEPES, 5 TEA-Cl, 0.4 EGTA, 4 Mg-ATP, 0.3 Na-GTP, 10 phosphocreatine, and 0.2 Alexa-594 (for visualizing dendritic morphology; Life Technologies); pH ~7.2. See *Subcellular LiGABAR Mapping via Two-photon GABA Uncaging* below for details about two-photon imaging and RuBi-GABA photolysis.

IPSC recordings in hippocampal neurons. Slices were placed in a recording chamber mounted on an upright fixed-stage microscope (MOM, Sutter) with gradient contrast IR optics (Siskiyou) and GFP epifluorescence. Slices were perfused with aCSF at room temperature at 1–2 mL/min. ACSF contained (in mM): 126 NaCl, 2.5 KCl, 1.25 NaH_2PO_4, 10 Glucose, 1.3 $MgCl_2$, 26 $NaHCO_3$ and 2.5 $CaCl_2$, equilibrated with 95% O_2 + 5% CO_2. Whole-cell recordings were made from GFP-positive CA1 pyramidal cells with glass microelectrodes (R = 4–7 MΩ) filled with internal solution containing (in mM): 108 Cs-gluconate, 2.8 NaCl, 20 HEPES, 5 TEA-Cl, 0.4 EGTA, 4 Mg-ATP, 0.3 Na-GTP and 10 phosphocreatine, adjusted to ~ 7.2 pH and ~290 mOsm. To record isolated IPSCs, 25 µM DNQX and 50 µM D-AP5 were added to the aCSF and cells were held at the reversal potential of excitatory inputs (0 mV). A glass stimulating electrode (filled with aCSF) was placed in proximal stratum radiatum ~100 µm away from the recorded cell. Synaptic responses were evoked by a 0.2-ms, 10–100 µA current pulse delivered via a stimulus isolation unit (AMPI). Conditioning light (390 nm or 540 nm) was generated by a Spectra-X light engine under software control (Lumencor) and delivered through the microscope objective. Membrane currents were amplified (Axopatch; Molecular Devices), digitized (Digidata; Molecular Devices) and recorded (pClamp; Molecular Devices) to a desktop computer.

Current-clamp recordings in hippocampal neurons. Whole-cell recordings from hippocampal neurons (in aCSF, without AP5 and DNQX) were performed using the instrumental setup described above. The internal solution contained (mM): 116 K-Gluconate, 6 KCl, 2 NaCl, 20 HEPES, 0.5 EGTA, 4 Mg-ATP, 0.3 Na-GTP and 10 phosphocreatine, adjusted to ~ 7.2 pH and ~290 mOsm. Conditioning light (390 nm or 540 nm) was applied 100 ms prior to Schaffer-collateral stimulation, with the recorded neuron at rest (around –70 mV). The stimulating electrode was placed in stratum radiatum ~400 µm from the recorded cell in CA1, and the stimulation was carried out at 0.5 Hz.

IPSC recordings in cortical and cerebellar neurons. Voltage-clamp recordings (V_{hold} = 0 mV) were made on cortical or cerebellar neurons at room temperature. Pipettes were pulled from filamented borosilicate glass with an open-tip resistance of 1.5–2.5 MΩ for cerebellar Purkine cells and of 3–5 MΩ for other neuron types. The internal solution contained (in mM): 108 Cs-gluconate, 2.8 NaCl, 20 HEPES, 1 EGTA, 5 TEA-Cl, 4 Mg-ATP, 0.4 Na-GTP; pH. 7.3. Synaptic currents were amplified by Axoclamp 200A or Multiclamp 700B (Molecular Devices),

recorded via pClamp 9.2/10 (Molecular Devices) or custom routines written with Matlab (Mathwork), and then filtered at 2 kHz and digitized at 10–20 kHz using a Digidata 1330/1440 (Molecular Devices) or BNC2090 (National Instrument) analog-to-digital convertor. Monosynaptic IPSCs were evoked using patch pipette filled with aCSF placed 1–200 μm away from the soma of the recorded neuron, with glutamatergic activities blocked by 3–4 mM kynurenic acid (Abcam). A constant current stimulus isolation unit was used (AMPI, Israel). Stimulus intensity was set between 250-750 μA to limit evoked IPSC amplitude below 750 pA. No correlation between the IPSC size and photoswitching magnitude were found (n = 6, Pearson correlation R= 0.77). LiGABAR photo-control was carried out using one of the following light sources: Polychrome (TILL Photonics), 380 nm (1 mW/cm^2) and 500 nm (1.6 mW/cm^2) delivered through a 4x objective; Spectra (Lumencor), 390 nm (3.5 mW/cm^2) and 540 nm (15 mW/cm^2) delivered through a 20x objective; Prizmatix (Prizmatix, Israel), 385 nm (20 mW/cm^2) and 500 nm (15 mW/cm^2) delivered through optic fibers with 1-mm core diameter.

Effects of PTL treatment on endogenous ion channels. Control experiments in Figures S3A, C, D, E, F were performed on hippocampal CA1 pyramidal cells in acute slices, which were prepared from wild-type Sprague-Dawley rats (P14–21) and treated with PAG-1C. IPSCs were evoked with electrical stimulation in *stratum pyramidale* and recorded in whole-cell voltage-clamp mode at 0 mV, with $GABA_B$ activities and glutamatergic inputs blocked with 5 μM CGP 54626, 10 μM DNQX, and 50 μM AP5. AMPAR-EPSCs were evoked with stimulation in *stratum radiatum* and recorded at –60 mV in the presence of 5 μM CGP 54626 and 100 μM picrotoxin to block all GABAergic activities. NMDAR-EPSCs were evoked with stimulation in *stratum radiatum* and recorded at +40 mV in the presence of 5 μM CGP 54626, 100 μM picrotoxin, and 10 μM DNQX. Voltage-gated sodium currents were evoked with a 200-ms step from –60 mV to –10 mV. Voltage-gated potassium currents were evoked with a 200-ms step from –60 mV to +40 mV in the presence of 3 μM TTX. Slices were perfused with aCSF at room temperature. Pipette solution for recording IPSCs, EPSCs, and sodium currents comprises (in mM): 108 Cs-gluconate, 2.8 NaCl, 20 HEPES, 5 TEA-Cl, 0.4 EGTA, 4 Mg-ATP, 0.3 Na-GTP and 10 phosphocreatine, adjusted to ~ 7.2 pH and ~290 mOsm. Pipette solution for recording potassium currents comprises (in mM): 116 K-Gluconate, 6 KCl, 2 NaCl, 20 HEPES, 0.5 EGTA, 4 Mg-ATP, 0.3 Na-GTP and 10 phosphocreatine, adjusted to ~ 7.2 pH and ~290 mOsm. GIRK-channel currents (for the measurement of $GABA_B$-receptor activation; Figure S3B) were evoked by applying 10 μM (*R*)-baclofen onto PAG-1C treated cultured hippocampal neurons. Whole-cell currents were recorded at room temperature with neurons held at –70 mV. The extracellular solution contained (in mM): 119.5 NaCl, 20 KCl, 1.2 $MgCl_2$, 2.5 $CaCl_2$, 5 HEPES, 10 Glucose, 0.025 DNQX, 0.05 AP5, and 0.001 TTX; pH 7.4. The intracellular solution contained (in mM): 10 NaCl, 135 K-gluconate, 2 $MgCl_2$, 10 HEPES, 2 Mg-ATP, 0.35 NaGTP, and 1 EGTA; pH 7.2.

In vivo Electrophysiology

Targeted-cell loose-patch recordings for Figure 6 were made from PV-tdTOM and LiGABAR-eGFP double positive cells in layer 2/3 (150–350 μm below pia) of the visual cortex using a two-photon laser scanning microscope (Sutter) with a Ti:Sapphire laser (Coherent) at 1050 nm. Two-photon images were acquired using Scanimage (Pologruto et al., 2003). Patch electrodes (4–5 MΩ) were filled with HEPES-aCSF and 50 μM Alexa Fluor 594 hydrazide (Invitrogen) for

visualization. Neuron spiking activities were recorded as action potential currents, with neurons being clamped at the voltage that generated zero holding current (using Multiclamp 700B amplifier with custom routines written with Matlab). Data were filtered at 2 kHz and digitized at 20 kHz using BNC2090 analog-to-digital convertor (National Instrument). For multi-electrode extracellular recordings in awake knock-in mice (Figure 8), we used 16-channel probe (NeuroNexus, A1x16-3mm-25-177-A16) to record neuronal activities. Recordings were amplified, digitized at 30 kHz (Spikegadget), and stored on a computer hard drive. MClust (http://redishlab.neuroscience.umn.edu/MClust/MClust.html) was used for off-line sorting of the spike waveforms.

Visual stimulus was either a circular patch of drifting square-wave gratings in full contrast (Figure 6) or a square full contrast checkerboard (Figure 8) against a mean luminance grey background. Gratings were presented at a temporal frequency of 2 Hz and a spatial frequency of 0.04 cycles/degrees (uncorrected for angle of monitor). Checkerboards (12.5 degrees per square) were presented 10 times for 100 ms at 2 Hz per episode. Stimuli were generated with PsychToolbox and presented on a gamma-corrected 20" or 23'' LCD screen with a 60 Hz refresh rate, ~15 cm from the mouse, oriented ~60 degree with respect to the body axis of the mouse.

Subcellular LiGABAR Mapping via Two-photon GABA Uncaging

Imaging and uncaging were performed using a two-photon laser scanning microscope (MOM; Sutter) with a 20x objective (0.95 NA; Olympus). The light source for fluorescence excitation (1.6 W, 140 fs pulses, 90 MHz, 800 nm for Alexa Fluor 594 and 940 nm for GFP-fused gephyrin intrabody) was a Ti:Sapphire laser (Chameleon XR; Coherent). The same light source was used for RuBi-GABA uncaging. Intensity was controlled by a Pockels cell (Conoptics). Imaging and uncaging were controlled by MScan software (Sutter). LiGABAR-expressing hippocampal neurons were voltage clamped at 0 mV, with 25 µM DNQX, 50 µM D-AP5, and 0.5 µM TTX. Internal solution included 200 µM Alexa Fluor 594 (Life Technologies) for visualizing dendritic morphology. RuBi-GABA (200-400 µM; Abcam) was added to aCSF and re-circulated using a peristaltic pump (Idex). Baseline laser power was adjusted to excite Alexa Fluor 594 without uncaging RuBi-GABA (~2 mW). Scan mirror location and laser intensity were controlled with MScan to uncage at designated locations for 5–10 ms at ~150 mW. Full-field 390 nm (1.2 mW/mm^2) or 540 nm (3.2 mW/mm^2) conditioning flashes (5 s) were generated by a Spectra-X light engine under software control (Lumencor) and delivered through the objective. After each flash, a 2-min rest period allowed the uncaged GABA to diffuse away (Figure S4). Because a *trans*-antagonist was used for both α1- and α5-LiGABARs, the receptors were antagonized by 540 nm and restored by 390 nm flashes, respectively. Photoswitching was thus calculated as $1 - (I_{540}/I_{390})$, where I refers to the peak amplitude of GABA-elicited current.

Immunocytochemistry

After being deeply anesthetized with ketamine and xylazine, wide-type and homozygote littermates of α1T125C knock-in mice (P30–P45) were perfusion-fixed with 2% paraformaldehyde in 0.1 M sodium acetate buffer (pH. 6) and post-fixed in the same solution for 2–4 h. The brains were transferred to 30% sucrose in 0.9% saline overnight for cryoprotection.

Sagittal sections (40 μm) were sliced using a microtome. Free-floating slices were incubated with TBS (0.05 M Tris and 0.15 M NaCl; pH 7.4) containing 10% normal goat serum (NGS, Jackson ImmunoResearch) for 1 h at room temperature. After blocking, slices were incubated with mouse anti-$GABA_AR$ α1 (diluted 1:500; NeuroMAB, UC Davis) in TBS with 2% NGS and 0.1% Triton X-100 at 4 ˚C overnight. After three washes with TBS, slices were incubated with Alexa 594-conjugated secondary goat anti-mouse antibody (1:500; Invitrogen) in TBS for 1 h at room temperature. After washing off residual secondary antibody, slices were mounted with anti-fade reagent (Vectorshield; Vector Labs). Digital images were acquired using a 0.64x objective (NA, 0.15) on an Olympus MVX10 stereomiscroscope using a LED light source (Lumencor) with filter sets of 535–555 nm for excitation and 570–625 nm for emission to collect Alexa-594 fluorescence.

The fluorescence intensity data in Figure 7 were measured using a 10-pixel width line (region of interests, ROI) drawing across to the anatomical landmarks on both the images from wide-type and knock-in brain sections. 2–4 measurements were made in each section for 2–3 sections from 2 animals of each genotype. Data were processed and analyzed using ImageJ.

Data Analysis

The electrophysiology data were analyzed in Clampex 10.2 (Molecular Device), Axograph X (AxoGraph) or customized routines in Matlab (Mathworks).

The dose-response curves in Figures 1D and S2 were measured using the following procedure. For each cell, the current elicited by each tested concentration was first normalized to a reference current elicited at ~EC_{50} (to correct for any possible drift in responses during the course of experiment). The normalized responses were then fitted by Hill Equation: $I/I_{max} = 1/(1 + (EC_{50}/[GABA])^n)$, where I represents the current amplitude elicited by the given [GABA], I_{max} represents the saturating response, EC_{50} is the [GABA] producing the half-maximal response, and n is the Hill coefficient. The GABA EC_{50} and Hill coefficient for each tested receptor were calculated as mean ± SEM from several analyzed cells. For group data presentation and fitting in Figures 1D and S2, the initially normalized responses were further scaled (to fall between 0 and 1) using the I_{max} of each cell as reference. Note that in Figure 1D, the Hill coefficient is reduced when α1-LiGABAR is illuminated with 500 nm light (0.64 ± 0.05, compared to 1.3 ± 0.1 with 380 nm and 1.3 ± 0.1 of the wild-type). This is likely due to incomplete PTL conjugation, which would result in a mixed population of fully and partially antagonized receptors.

Representative IPSC traces shown in Figures 3 and 7 are the average from 5–10 individual traces. For curve fitting in Figures 4C, 5C and 5F, we performed single exponential fit y = a*exp(b*x) to derive the time and depth constants in Matlab. We reported 95% confidence bounds value as the statistics of the goodness of fit. In Figures 5 C and 5F, the maximal photoswitching was estimated from the y-intercept of the fit through back-extrapolation. All the data points were then normalized to the maximum value to construct the plots.

In Figure 6, we used a threshold method for spike detection. The minimum threshold used was 4 times of the standard deviation of the baseline noise. PSTH plot was constructed with bin size of 25 ms.

Multi-electrode recording data (Figures 8 and S7) were analyzed in Matlab. Spike waveforms were sorted into clusters off-line using MClust using features of peak, trough, energy and time of the waveforms. We accepted clusters as single units if the cluster has less than 1.4% of the waveforms inter-spike intervals < 2 ms and was well separated from noises with its cluster separation distance > 5 (Schmitzer-Torbert et al., 2005). Waveforms were interpolated with cubic splines by a factor of 100 and spike half width and asymmetry index were extracted. The spike width is defined as the time from trough to the 2nd peak. The asymmetry index is defined as: $(A_1 - A_2)/(A_1 + A_2)$, where A_1 and A_2 are the amplitude of the first and second peak, respectively (bottom left inset, Reyes-Puerta et al., 2015). Fast spike and regular spiking units are classified by *k*-means clustering for spike half width and asymmetry index (Figure S7). Average firing rates and average power of the local field potential (20–60 Hz) in each of the total 40 episodes were tested with Friedman tests to determine significance of modulation by conditioning light. In the PTL treated knock-in mice, only mice with significant change in both single unit firing rates and gamma power were included in the results (3 out of 5 mice, one mouse showed no firing rate change and one mouse showed no gamma change). In vehicle-treated knock-in mice, each of the 2 mice received 2 recording sessions with the probe placed at 2 different locations around the injections site.

Imaging data were processed and analyzed using ImageJ. Statistics were performed using Microsoft Excel, GraphPad, and Matlab.

Supplemental References

Connolly, C.N., Krishek, B.J., McDonald, B.J., Smart, T.G., and Moss, S.J. (1996). Assembly and cell surface expression of heteromeric and homomeric gamma-aminobutyric acid type A receptors. J. Biol. Chem. *271*, 89–96.

Kugler, S., Kilic, E., and Bahr, M. (2003). Human synapsin 1 gene promoter confers highly neuron-specific long-term transgene expression from an adenoviral vector in the adult rat brain depending on the transduced area. Gene Ther. *10*, 337–347.

Lin, W.-C., Davenport, C.M., Mourot, A., Vytla, D., Smith, C.M., Medeiros, K.A., Chambers, J.J., and Kramer, R.H. (2014). Engineering a light-regulated $GABA_A$ receptor for optical control of neural inhibition. ACS Chem. Biol. *9*, 1414–1419.

O'Mara, M. Cromer, B., Parker, M., and Chung, S. –H. (2005). Homology model of the $GABA_A$ receptor examined using Brownian Dynamics. Biophys. J. *88*, 3286–3299.

Pologruto, T.A., Sabatini, B.L., and Svoboda, K. (2003). ScanImage: flexible software for operating laser scanning microscopes. Biomed. Eng. Online *2*, 13.

Reyes-Puerta, V., Sun, J.J., Kim, S., Kilb, W., and Luhmann, H.J. (2015). Laminar and columnar structure of sensory-evoked multineuronal spike sequences in adult rat barrel cortex in vivo. Cereb. Cortex *25*, 2001–21.

Schmitzer-Torbert, N., Jackson, J., Henze, D., Harris, K., and Redish, A.D. (2005). Quantitative measures of cluster quality for use in extracellular recordings. Neuroscience *131*, 1–11.

Tretter, V., Jacob, T.C., Mukherjee, J., Fritschy, J.-M., Pangalos, M.N., and Moss, S.J. (2008). The clustering of $GABA_A$ receptor subtypes at inhibitory synapses is facilitated via the direct binding of receptor α2 subunits to gephyrin. J. Neurosci. *28*, 1356–1365.

Wotring, V.E., Chang, Y., and Weiss D.S. (1999). Permeability and single channel conductance of human homomeric ρ1 $GABA_C$ receptors. J. Physiol. *521*, 327–336.